Available online at www.sciencedirect.com
ScienceDirect
Journal of Magnetic Resonance 186 (2007) 238–242
JMR Journal of Magnetic Resonance
www.elsevier.com/locate/jmr

Tailored slice selection in solid-state MRI by DANTE under magic-echo line narrowing

Shigeru Matsui [a,b,*], Hidefumi Masumoto [b], Takeyuki Hashimoto [c]

[a] Institute of Applied Physics, University of Tsukuba, Tsukuba, Ibaraki 305-8573, Japan
[b] Graduate School of Pure and Applied Sciences, University of Tsukuba, Tsukuba, Ibaraki 305-8573, Japan
[c] Department of Information Technology, Yokohama Soei Junior College, Yokohama, Kanagawa 226-0015, Japan

Received 25 December 2006; revised 7 March 2007
Available online 16 March 2007

Abstract

We propose a method of slice selection in solid-state MRI by combining DANTE selective excitation with magic-echo (ME) line narrowing. The DANTE RF pulses applied at the ME peaks practically do not interfere with the ME line narrowing in the combined ME DANTE sequence. This allows straightforward tailoring of the slice profile simply by introducing an appropriate modulation, such as a sinc modulation, into the flip angles of the applied DANTE RF pulses. The utility of the method has been demonstrated by preliminary experiments performed on a test sample of adamantane.
© 2007 Elsevier Inc. All rights reserved.

Keywords: Slice selection; MRI; DANTE; Magic echo; Line narrowing

1. Introduction

The method of slice selection is well-established in liquid-state MRI. The sinc-shaped soft RF pulse applied in the presence of a field gradient achieves the nearly ideal slice selection. This selection scheme, however, does not work in solid-state MRI where the transverse relaxation time T_2 of the object is much shorter than the soft RF pulse. Although a few slice selection methods have been proposed for solid-state MRI [1–3], each method suffers from its own problem: the method relying on spin locking in the presence of a field gradient exhibits a relatively poor selectivity [1]. The generalized DANTE method combined with multiple-pulse line narrowing is technically demanding [2]. The method using off-resonance spin tipping selects a slice necessarily in the form of longitudinal magnetization [3]. Furthermore, in all the methods proposed so far, the shape of the slice profile is uniquely determined by the method employed and cannot be tailored by the experimenter. These drawbacks seem to have hampered their widespread use in solid-state MRI.

Here, we describe a simple slice selection method for solid-state MRI by combining DANTE selective excitation [4] with magic-echo (ME) line narrowing [5–15]. The new method is technically less demanding, selects a slice in the form of transverse magnetization, and permits tailoring the shape of the slice profile for the first time in solid-state MRI.

2. The ME DANTE method

The original DANTE sequence developed for NMR spectroscopy consists of regularly spaced N short RF pulses. The on-resonance flip angle of each pulse is defined by α_i ($i = 1, 2, 3, \ldots, N$). All the flip angles are identical and the sum of the flip angles is fixed at 90° (Fig. 1). During the pulse spacing τ_D, free precession occurs, leading to the frequency-dependent RF excitation. Since the frequency dependence can be converted to the spatial dependence

* Corresponding author. Address: Institute of Applied Physics, University of Tsukuba, Tsukuba, Ibaraki 305-8573, Japan. Fax: +81 29 853 5205.
E-mail address: matsui@bk.tsukuba.ac.jp (S. Matsui).

1090-7807/$ - see front matter © 2007 Elsevier Inc. All rights reserved.
doi:10.1016/j.jmr.2007.03.005

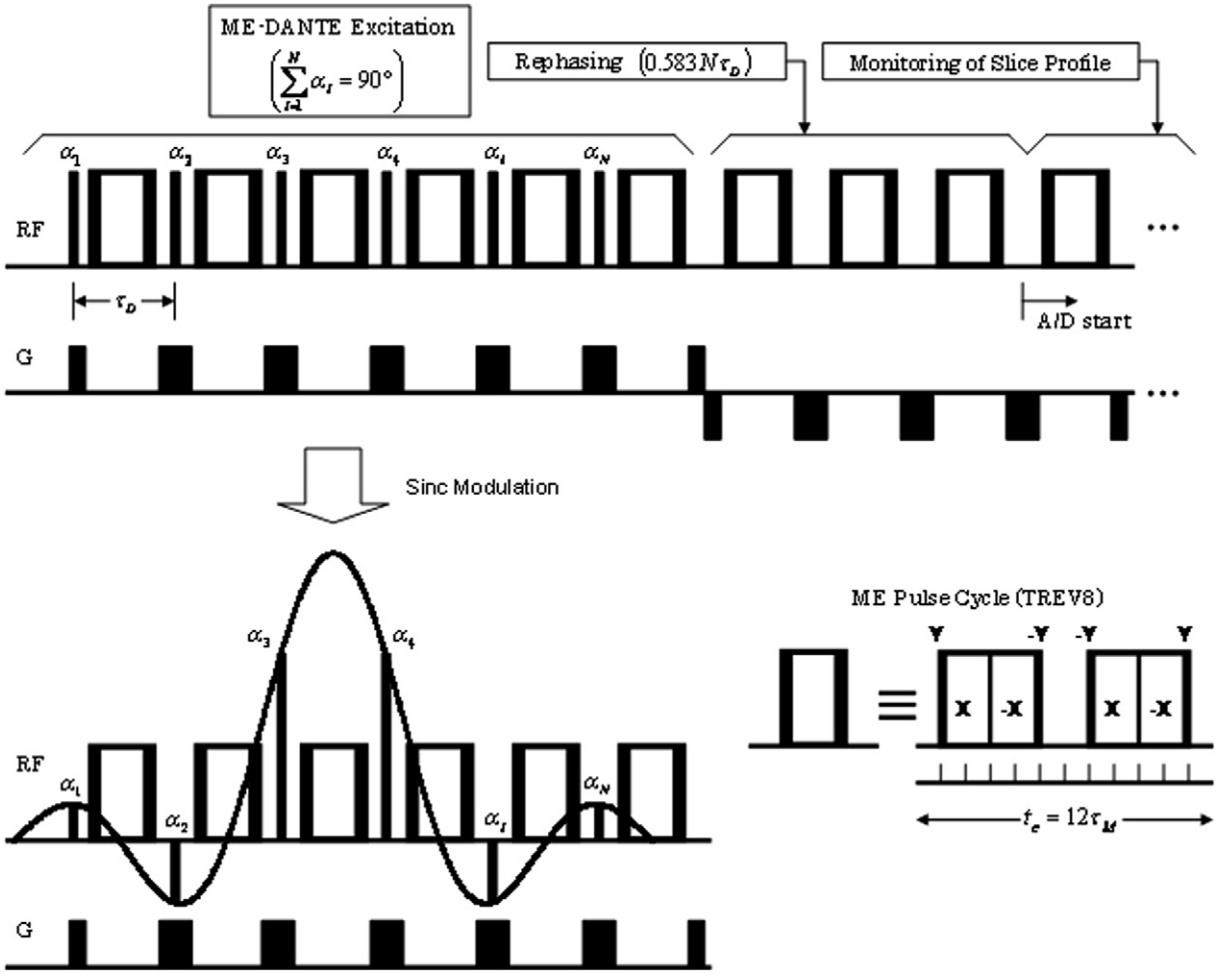

Fig. 1. Pulse sequences for the ME DANTE method of slice selection in solid-state MRI. The sequences comprise two time intervals of ME DANTE excitation and rephasing (for 0.583 $N\tau_D$), followed by the additional sequence for monitoring the profile of the selected slice. Upper sequence: the original DANTE sequence consisting of N identical hard RF pulses (α_i; $i = 1, 2, 3, \ldots, N$) is combined with the ME line narrowing sequence. The DANTE RF pulses are applied at ME peaks every pulse cycle of TREV8 ($\tau_D = t_c$) so as to avoid their interference with the ME line narrowing. Lower sequence: a sinc modulation is introduced into the DANTE sequence by changing the flip angles appropriately for tailoring the slice profile. Field gradient pulses G are applied for transforming the frequency response of the DANTE sequence to the spatial response. The gradient pulses are inverted during the second time interval for rephasing by means of gradient echo. In the middle of the pulse cycle TREV8, signal sampling is made and a gradient pulse is applied despite not indicated explicitly. The α_i pulse amplitudes are depicted exaggerated; the maximum amplitude is the same as that of 90° pulses in the ME sequence.

by application of a field gradient G, slice selection can be attained by the DANTE sequence.

The regular spacing of the DANTE hard-pulse sequence makes it ideally suited for the combination with the ME sequence which is cyclic. For combining the DANTE sequence with the ME line narrowing sequence without lowering the line narrowing efficiency, it is necessary to apply the DANTE RF pulses at the ME peaks where the time evolution of the spin system is free from the dipolar interaction. This point is discussed below in comparison with similar approaches employing the multiple pulse sequences for line narrowing.

The combined ME DANTE pulse sequence is represented by the upper sequence in Fig. 1. The field gradient pulses G are applied for the conversion from the frequency to the spatial discrimination. The ME DANTE excitation is followed by the ME sequence with reversed gradient pulses for rephasing the signal, similarly as in the soft RF pulse excitation commonly used for liquid-state MRI [16]. The optimal rephasing was evaluated by numerical simulation based on the Bloch equations [16]. It has been found that the rephasing can be optimized by reversing the gradient G for 0.583 $N\tau_D$ following the excitation (Fig. 1). (We did not employ the analytical expression [17] for the simulation because the numerical simulation was more suitable for evaluating the optimal rephasing.) The rephased signal is then detected by the 1D ME imaging sequence (A/D start) for monitoring the slice profile. The TREV8 [6] was employed as the ME pulse cycle, since it is compact and exhibits a reasonably good line-narrowing efficiency. The cycle time $t_c = 12\tau_M$ was set equal to the DANTE pulse spacing τ_D. All the DANTE RF pulses are applied along the x axis in the rotating frame.

We note here that similar DANTE approaches to slice selection are conceivable by employing the multiple pulse sequences such as MREV8 for line narrowing. However, the DANTE RF pulses directly inserted into the multiple pulse sequence are expected to interfere with the coherent averaging of the dipolar interaction, leading to a lowered line-narrowing efficiency [18]. Consequently, Caravatti et al. devised a special multiple pulse sequence called a "permuted pulse cycle" to accommodate the DANTE selectivity with minimal line-narrowing deficiency [18]. Another combination of the multiple-pulse line narrowing with the DANTE was also demonstrated as mentioned in Section 1 [2], where the problem of interference was solved by utilizing a generalized DANTE sequence. The DANTE sequence can be generalized by regarding it as alternative rotations about the two mutually perpendicular axes. On the other hand, the problematic interference can be minimized simply by application of the DANTE RF pulses at the ME peaks in the ME DANTE approach.

It is important to note that by introducing an appropriate modulation into the inserted DANTE RF pulses as indicated by the lower sequence in Fig. 1, one can readily tailor the shape of the slice profile. The sinc modulation leads to an ideal rectangular shape. This ability of straightforward tailoring can be brought about by the negligibly small interference obtained in the ME DANTE approach, as will be verified by our ME DANTE experiments.

3. Results and discussion

Fig. 2 shows the results of the ME DANTE experiments performed on the adamantane test sample in a tube of inner diameter 7 mm. Slice profiles monitored by the 1D ME imaging sequence are displayed. The DANTE pulse spacing τ_D was set at 360 μs. Due to the restricted capability of our pulse generator used in all the experiments, the number of DANTE RF pulses N was limited to 6. Profile 2a represents the 1D spin density image obtained by nonselective 90 °pulse excitation. Profile 2b was obtained by the ME original DANTE experiment. Since all the flip angles α_i ($i = 1, 2, 3, \ldots, 6$) were set equal to 15° (Fig. 1, upper sequence), the well-known sinc-shaped profile is observed. Profiles 2c and 2d were acquired by the ME sinc-modulated DANTE experiments. The sinc modulations employed are represented by the flip angles $\alpha_1 = \alpha_6 = 10.4°$, $\alpha_2 = \alpha_5 = -17.3°$, and $\alpha_3 = \alpha_4 = 51.9°$ for profile 2c (Fig. 1, lower sequence) and $\alpha_1 = \alpha_6 = 4.8°$, $\alpha_2 = \alpha_5 = 16.1°$, and $\alpha_3 = \alpha_4 = 24.1°$ for profile 2d.

The presence of the negative peaks of the 1st sidebands at both ends of profiles, which were inverted as a result of

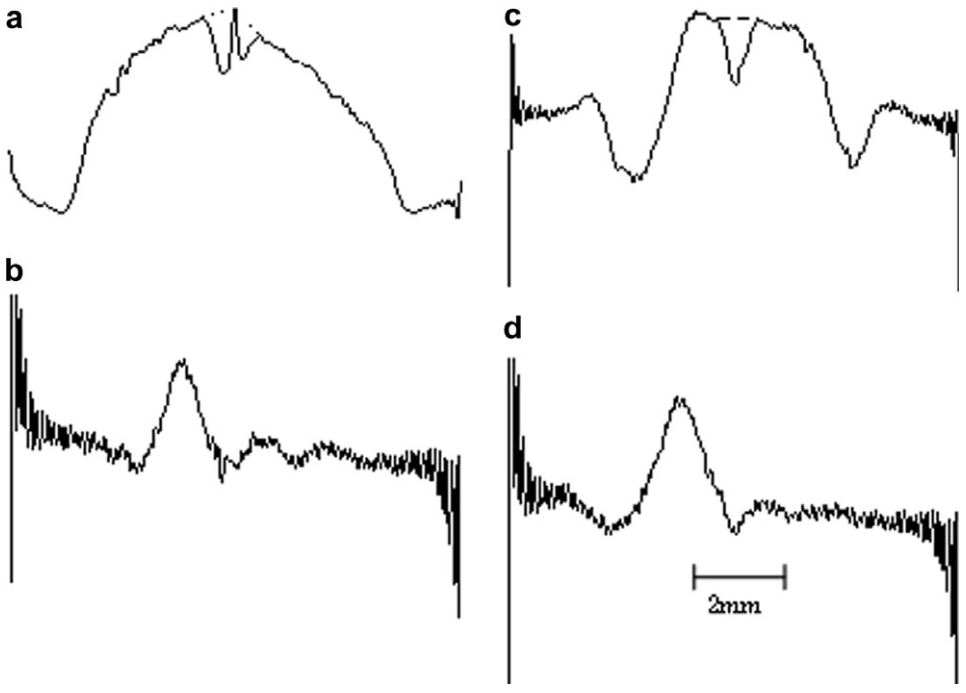

Fig. 2. ME DANTE experimental results obtained on an adamantane sample. The sample was in a tube of inner diameter 7 mm. (a) 1D spin density image obtained by nonselective 90 °pulse excitation. (b) The sinc-shaped slice profile obtained by the ME original DANTE experiment (upper sequence in Fig. 1, $N = 6$). (c) The slice profile observed by the ME DANTE experiment employing the sinc modulation represented by the flip angles of the pulses $\alpha_1 = \alpha_6 = 10.4°$, $\alpha_2 = \alpha_5 = -17.3°$, and $\alpha_3 = \alpha_4 = 51.9°$ (lower sequence in Fig. 1, $N = 6$). (d) The slice profile acquired by the ME DANTE experiment using the sinc modulation represented by the flip angles $\alpha_1 = \alpha_6 = 4.8°$, $\alpha_2 = \alpha_5 = 16.1°$, and $\alpha_3 = \alpha_4 = 24.1°$. Note that the shape of profile (c) (positive portion) is close to a rectangle. Also, the sidelobes accompanying the thinner slice in profile (d) are much smaller than those of the slice in profile (b). These results indicate that the ME DANTE method works well. The profiles, however, suffer from artifacts such as a dip in the profile center and beat patterns on both ends. Nevertheless, the artifacts can be mainly ascribed to the ME imaging process for profile monitoring (see text for further details). The peaks in profiles (b) and (d) are intentionally shifted to the left. The reduced amplitudes in profiles (b–d) relative to profile (a) are due to the transverse relaxation during the ME DANTE excitation and rephasing.

the optimal rephasing, complicates the appearance of profile 2c. However, it can be seen that the shape of the center-band slice profile (positive portion) is close to a rectangle. Also, the sidelobes accompanying the thinner slice obtained in profile 2d are much smaller than those of the slice in profile 2b. The slice thickness in profile 2c is one half the FOV of about ±4.8 mm and it is three times thicker than that in profile 2d. These results clearly demonstrate that the experiments of ME DANTE excitation work well.

All the profiles, however, suffer from at least either of two types of artifacts, a dip in the center and beat patterns on both ends. The dip in profile 2a contains a sharp peak inside. Nevertheless, these artifacts may result mainly from the monitoring ME sequence as will be discussed below. The central peaks are intentionally shifted to the left in profiles 2b and 2d to avoid the dip artifact. The small asymmetry observed in profiles 2a and 2c with respect to the profile center may be ascribed to the nonlinearity in the field gradient.

The results in Fig. 2 also confirm that the DANTE RF pulses do not significantly interfere with the ME line narrowing. The virtual absence of such interference, however, can be more directly confirmed by the fact that the amplitudes of profiles 2b–d are reduced to about one half, compared to that of profile 2a: the transverse relaxation time of the adamantane sample has been prolonged by the ME line narrowing from 50 μs to 3.5 ms. The reduction factor 1/2 can be well explained by assuming the transverse relaxation time of 3.5 ms in the numerical simulation. The DANTE interference with the ME line narrowing during the ME DANTE excitation is thus practically absent.

We briefly discuss the two types of artifacts in Fig. 2, a dip in the center and beat patterns on both ends. It can be recognized that the dips in profiles 2a and 2c appear roughly the same except the sharp peak inside in profile 2a. This strongly suggests that this artifact results mainly from the ME monitoring and the contribution from the ME DANTE excitation and the rephasing process is relatively small. The sharp peak inside the dip in profile 2a may be due to the spin locking effect of the ME sequence [19]; however, such effect would be suppressed largely by the DANTE RF pulses inserted into the ME sequence in profile 2c. It is most likely that the dip may be generated by the abruptly decreased efficiency of the line narrowing around the center where the second averaging is ineffective [20]. It was confirmed experimentally by the offsetting that the shapes of the peaks which can be observed if the dip artifacts are absent in profiles 2a and 2c, would be as corrected by the broken line.

The beat patterns on both ends are due to the fact that the signal sampling (A/D) was made twice the cycle time t_c for doubling the FOV to accommodate properly the thick slice of profile 2c. (This is not shown explicitly in Fig. 1.) As is well-known [8], this over-sampling gives rise to producing a peak with many sidelobes at the Nyquist frequencies, i.e. at both ends. In fact, the beat patterns could be removed by making the signal sampling once the cycle time t_c. Therefore, the beat patterns can entirely be ascribed to the monitoring ME sequence.

4. Conclusions

We have proposed the slice selection method for solid-state MRI by combining DANTE with the ME line narrowing. It has been confirmed that the DANTE RF pulses inserted into the ME sequence do not significantly interfere with the ME line narrowing. The preliminary experiments have demonstrated that the ME DANTE method with the sinc modulation can be useful for slice selection in MRI of solids. Due to the limited number of DANTE RF pulses $N = 6$, the sufficiently thin slice with a rectangular profile could not be obtained. For obtaining a thinner slice, the number N must be increased. Additional experiments for improving the performance of the ME DANTE method are currently in progress.

Finally, it should be pointed out that the tailoring ability of the ME DANTE method would be useful not only for the slice selection in solid-state MRI but also for the selective excitation in high-resolution NMR spectroscopy of solids [18,21].

5. Experimental

All the experiments were performed on a homebuilt NMR imager, operating at 59.85 MHz for protons. The width of the 90° pulses in the ME sequence was 2.4 μs. The flip angles of the DANTE RF pulses were adjusted as follows: the RF pulses with the largest flip angle were obtained by reducing the pulse width while keeping the amplitude same as that of the 90° pulses. Then, the flip angles of the other RF pulses were adjusted by reducing the amplitudes without changing the pulse width. The actual RF pulse widths were fixed to 0.4, 1.4, and 0.6 μs for Fig. 2b–d. We noticed no problems with the finite pulse widths. This is presumably due to the fact that the pulse widths were short enough for the adamantane sample. The adamantane sample contained in the tube was about 5 mm long, and its relaxation times were $T_1 \sim 1$ s and $T_2 = 50$ μs. The T_2 of adamantane was prolonged to 3.5 ms by the ME line narrowing. A field gradient of 41 mT/m was applied perpendicular to the tube axis.

In the ME monitoring, typically 80 points were sampled every 180 μs and zero-filled to 256 points prior to the Fourier transformation, giving a resolution of approximately 100 μm. Twenty signals were accumulated to improve the signal-to-noise ratio in the ME DANTE experiments.

Acknowledgments

We thank the late Professor Tamon Inouye of University of Tsukuba for encouragement. Thanks are also due to Institute for Applied Mathematics, Inc., for financial support.

References

[1] R.A. Wind, J.H.N. Creyghton, D.J. Ligthelm, J. Smidt, Spatial selection in NMR by spin-locking, J. Phys. C: Solid State Phys. 11 (1978) L223–L226.

[2] D.G. Cory, J.B. Miller, A.N. Garroway, DANTE slice selection for solid-state NMR imaging, J. Magn. Reson. 90 (1990) 544–550.

[3] S. Matsui, Spatially selective excitation in solid-state NMR by off-resonance spin tipping, J. Magn. Reson. 97 (1992) 335–341.

[4] G. Bodenhausen, R. Freeman, G.A. Morris, A simple pulse sequence for selective excitation in Fourier transform NMR, J. Magn. Reson. 23 (1976) 171–175.

[5] W.-K. Rhim, A. Pines, J.S. Waugh, Time-reversal experiments in dipolar-coupled spin systems, Phys. Rev. B 3 (1971) 684–696.

[6] K. Takegoshi, C.A. McDowell, A "magic echo" pulse sequence for the high-resolution NMR spectra of abundant spins in solids, Chem. Phys. Lett. 116 (1985) 100–104.

[7] S. Matsui, Solid-state NMR imaging by magic sandwich echoes, Chem. Phys. Lett. 179 (1991) 187–190.

[8] S. Matsui, Suppressing the zero-frequency artifact in magic-sandwich-echo proton images of solids, J. Magn. Reson. 98 (1992) 618–621.

[9] S. Matsui, Y. Ogasawara, T. Inouye, Proton images of elastomers by solid-state NMR imaging, J. Magn. Reson. A 105 (1993) 215–218.

[10] S. Matsui, A. Uraoka, T. Inouye, Solid-state NMR imaging by tetrahedral-magic-echo time-suspension sequences, J. Magn. Reson. A 120 (1996) 11–17, and references therein.

[11] S. Matsui, S. Saito, T. Hashimoto, T. Inouye, NMR second moment imaging using Jeener–Broekaert dipolar signals, J. Magn. Reson. 160 (2003) 13–19, and references therein.

[12] F. Weigand, B. Blümich, H.W. Spiess, Application of nuclear magnetic resonance magic sandwich echo imaging to solid polymers, Solid State NMR 3 (1994) 59–66.

[13] M.L. Buszko, G.E. Maciel, Magnetic-field-gradient-coil system for solid-state MAS and CRAMPS NMR imaging, J. Magn. Reson. A 107 (1994) 151–157.

[14] M.A. Hepp, J.B. Miller, Mapping molecular orientation by solid-state NMR imaging, J. Magn. Reson. A 111 (1994) 62–69.

[15] G.S. Boutis, P. Cappellaro, H. Cho, C. Ramanathan, D.G. Cory, Pulse error compensating symmetric magic-echo trains, J. Magn. Reson. 161 (2003) 132–137.

[16] P.R. Locher, Computer simulation of selective excitation in n.m.r. imaging, Phil. Trans. R. Soc. Lond. B 289 (1980) 537–542.

[17] A. Sodickson, D.G. Cory, A generalized k-space formalism for treating the spatial aspects of a variety of NMR experiments, Prog. Nucl. Magn. Reson. Spectro. 33 (1998) 77–108, and references therein.

[18] P. Caravatti, M.H. Levitt, R.R. Ernst, Selective excitation in solid-state NMR in the presence of multiple-pulse line narrowing, J. Magn. Reson. 68 (1986) 323–334.

[19] S. Matsui, H. Miura, ^{1}H–^{13}C cross-polarization using a modified magic echo sequence for ^{1}H spin locking, Chem. Phys. Lett. 242 (1995) 163–168.

[20] D.G. Cory, J.B. Miller, A.N. Garroway, Multiple-pulse methods of ^{1}H N.M.R. imaging of solids: second-averaging, Mol. Phys. 70 (1990) 331–345.

[21] M. Hohwy, J.T. Rasmussen, P.V. Bower, H.J. Jakobsen, N.C. Nielsen, ^{1}H chemical shielding anisotropies from polycrystalline powders using MSHOT-3 based CRAMPS, J. Magn. Reson. 133 (1998) 374–378.